Acta Astronautica 82 (2013) 95–109

Contents lists available at SciVerse ScienceDirect

Acta Astronautica

journal homepage: www.elsevier.com/locate/actaastro

Behaviour based, autonomous and distributed scatter manoeuvres for satellite swarms

Sreeja Nag [a,b,*], Leopold Summerer [b]

[a] Department of Aeronautics and Astronautics, Massachusetts Institute of Technology, Cambridge, USA
[b] Advanced Concepts Team, European Space Agency (ESTEC), Noordwijk, The Netherlands

ARTICLE INFO

Article history:
Received 27 December 2011
Received in revised form
6 April 2012
Accepted 17 April 2012
Available online 22 June 2012

Keywords:
Swarm intelligence
Satellite clusters
Equilibrium shaping
Formation flying
Collision avoidance

ABSTRACT

One of the key requirements of a satellite cluster is to maintain formation flight among its physically distinct elements while at the same time being capable of collision avoidance among each other and external threats. This paper addresses the capability of clusters with tens and scores of satellites to perform the collision avoidance manoeuvre in the event of an external, kinetic impact threat, via distributed autonomous control and to return to its original configuration after the threat has passed. Various strategies for response manoeuvres are proposed based on a path planning scheme called "equilibrium shaping". The satellites in the cluster, modelled as a swarm of agents, follow biological rules of "avoidance" of each other and the threat, "gather" to maintain the formation cluster and "attraction" towards target location according to pre-defined artificial potential functions. The desired formation of this multi-agent system represents equilibrium points i.e., a minimum potential state, leading to predictable emergent behaviour for the entire cluster. The dynamical system is defined by adding a control feedback to the solution of the Hill–Clohessy–Wiltshire equations in order to track the desired velocities (as returned by the kinematic swarm model for equilibrium points). Various distributed path-planning, collision avoidance strategies are compared to each other in terms of the following metrics: delta-V spent during the manoeuvre, time required for the cluster to return to normal operations and distance of closest approach with the threat. Actuation and technological feasibility of the above strategies is benchmarked using available and potential CubeSAT system capabilities for propulsion, sensing and communication range. The significance of the results on designing future responsive, distributed space systems is discussed.

1. Introduction

A satellite constellation is a group of artificial satellites—a set of physically independent, "free-flying" modules that collaborate on—orbit to collectively achieve a certain level of system-wide functionality. They may communicate with each other, remain aware of each others' states, operate with shared control and complement each other in terms of overall functionality. A satellite cluster is a constellation that needs to maintain a certain amount of proximity between the physical elements and must fly in formation accordingly. Clusters may be homogenous or heterogeneous in form and/or function.

While each satellite in a cluster has traditionally been considered a self-sustaining entity in terms of the entire spacecraft bus (everything minus the payload), a new paradigm design in clusters called fractionated spacecraft allows for the distribution of almost all subsystems of a

* Corresponding author at: Department of Aeronautics and Astronautics, Massachusetts Institute of Technology, Cambridge, USA.
Tel.: +1 6177101845.
E-mail address: sreeja_n@mit.edu (S. Nag).

0094-5765/$ - see front matter © 2012 Elsevier Ltd. All rights reserved.
http://dx.doi.org/10.1016/j.actaastro.2012.04.030

satellite among the different physical elements. Each module in a fractionated spacecraft is composed of various subsystems, and thus a fractionated spacecraft might consist of separate modules responsible for power generation and storage, communications, payload, and so on. In 2008, DARPA in the USA began a programme called the System F6 Phase 1 (for Future, Fast, Flexible, Fractionated, Free-Flying Spacecraft) aiming to generate a new paradigm for space systems, especially in the responsive space sector [1,2]. The large, monolithic spacecraft of today is not designed for responsiveness and has other drawbacks (e.g., delay cascading in manufacturing), which a fractionated spacecraft approach could eliminate or reduce. This approach allows for quite a disruptive change in how satellites are built and how they will be used, since the establishing of space infrastructure lowers the entry barrier for satellite building and allows for resource sharing. The main idea is to modularize satellites up to the point where the monolithic spacecraft can be decomposed into a network of wirelessly linked modules, all separate smaller spacecraft, flown in a cluster and providing the same or more capabilities than a single spacecraft. The concept is assessed in [3] mainly regarding its influences on the aerospace sector, resulting from standardization and mass production. While DARPA's stress was on quantitative analysis of the fractionated spacecraft, the European Space Agency conducted a more qualitative analysis using an internal GSP study [4]. The options for fractionation for each of the subsystems were evaluated, given the current technological capabilities and strategies for networking and cluster dynamics proposed. Different fractionated architectures were benchmarked based on above analysis and 4 reference missions (LEO, GEO, Lagrange points and planetary missions). The study concluded that the system increases flexibility, reliability and is suitable for missions requiring continuity. On the other hand, it requires standardization of modules and is more vulnerable to kinetic impact of space debris. A fractionated spacecraft may therefore be considered a satellite cluster, heterogeneous in both form and function.

Taking into account the findings in literature that one of the chief drawbacks of satellite clusters and fractionated spacecraft is their vulnerability to impact, causing degradation or loss of a (possibly important) module, this paper addresses the problem of distributed evasive manoeuvres by the cluster's satellites, when approached by a kinetic threat.

2. Research motivation

One of the key requirements of a satellite cluster with multiple physical entities is the need for all the modules to fly within a tight ellipsoid in orbit in order to be functional. This requires solutions to multi-body problems in Earth orbit, precise determination of position, attitude and time, advanced control algorithms, trajectory planning and a host of other issues. There have been many instances of cluster formation flight. In the late 1990s, the US Air Force began the conceptual design of TechSAT-21, which was to demonstrate the ability of several satellites to replace a large monolith in an interferometric mission. Although the program was cancelled later, it provides a rich resource to literature on formation flight technology. NASA demonstrated Enhanced Formation Flying (EFF) via their first formation flight mission in 2000 called the Earth Observation 1 (EO-1), which flew in formation with LandSat-7, an Earth environment satellite launched in 1999. NASA's New Millennium Program, of which EO-1 was a part, was thus a great success and it paved the way to many technological FF milestones, which has now led to the plan of the Terrestrial Pathfinder Mission (TPF). In TPF, a virtual space interferometer system, with a 1 km baseline, will be implemented to detect and analyse the light from stars. NASA has also planned Magnetospheric Multi-Space (MMS) and Solar Imaging Radio Array (SIRA) as future formation flying missions. In 2002, the Gravity Recovery and Climate Experiment (GRACE) supported by NASA and DLR demonstrated formation flight by a pair of satellites to measure the Earth's gravity field and its temporal variations. The European Space Agency (ESA) has proposed the following formation flying projects: PROBA-3 with 3-axis stabilized pair of satellites [5], DARWIN to study the origins of life with one leader and 4 follower satellites and SWARM to study the Earth's magnetic field with 3 satellites.

In a space environment, that is getting increasingly crowded, another key requirement of satellite clusters is collision avoidance, from other satellites, orbital debris or even anti-satellite missiles. The US Space Surveillance Network is tracking more than 19,000 Earth-orbiting man-made objects more than 10 cm in diameter, of which roughly 95% are debris [6]. There are also an estimated 300,000 additional man-made objects in Earth orbit measuring 1–10 cm and more than a million smaller than 1 cm. In February 2009, a defunct Russian Cosmos satellite collided in space with a commercial Iridium satellite, not only causing destruction but also adding to the debris already present in space. In June 2007, NASA reported manoeuvring its $1.3 billion Terra satellite to avoid a piece of Fengyun-1C debris. Antisatellite (ASAT) missiles have been technologically demonstrated since 1960, when a US U-2 spy plane was destroyed by a USSR ASAT [7]. The US tested its Air-launched miniature vehicle (ALMV) in the early 1980s to demonstrate 'kinetic kill'. Thereafter, in spite of oscillating treaties such as the Outer Space Treaty (1967), Anti-Ballistic Missile Treaty (1972), the ban on ASAT testing (1986), the third generation ASAT systems were developed. Most recently, in 2007, China tested the kinetic kill technology of its ASAT system by shooting down its own satellite.

Collision avoidance has been discussed in past literature, although very rarely for completely distributed systems. The most popular approach has been linear programming where the obstacles and required formation is treated as a constraint, modelled using Mixed Integer Linear Programming (MILP) [8]. NASA's Jet Propulsion Laboratory published a collision avoidance approach based on the Bouncing Ball algorithm (BB) and Stalemate which adopts a heuristic approach to multiple satellite reconfigurations [9]. ESA's PRISMA satellites, developed under the contract to the Swedish Space Corporation, have robust collision avoidance algorithms for autonomous formation where separation and nominal guidance are solved for analytically. Analytical solutions are possible since the satellites have near-circular orbit [10,11]. Another approach of avoidance has been to propagate uncertainty covariances and calculate the probability that the relative displacement between two objects is less than a "collision metric" [12]. Princeton Satellite Systems has come up with distributed guidance laws for low, medium and high autonomy of constellations, solved using linear programming [13].

The above algorithms, are either centralized algorithms or assume the presence of a 'captain' to assess the distributed inputs from the less intelligent agents. Two unique collision avoidance techniques using distributed satellite systems were implemented at MIT in the Space Systems Laboratory. One technique used the artificial potential concept (APF) was used along with the Linear Quadratic Regulator (LQR) to demonstrate avoidance of both fixed and moving obstacles [14]. Velocities were modelled according to mathematical Gaussian functions centred at the target and obstacles. The other technique worked by predicting the closest point of approach and then overriding regular satellite controls to move the satellites in a direction perpendicular to the collision to avoid it [15]. Both theoretical concepts have been tested on a nano-satellite testbed called the SPHERES facility [16] developed by MIT SSL. While both pieces of work have suggested methods by which the algorithms can be scaled up to multiple satellites, none have demonstrated it for hundreds of satellites. If the algorithms were to be used for scores of satellites, implementations promise to scale up computationally and are further complicated if the cluster is heterogeneous.

Principles of swarm intelligence are currently being used to navigate decentralized groups of robots where each robot is treated like an intelligent agent that follows biological behavioural rules to maintain functionality. NASA is planning to use swarm intelligence in its ANTS mission to explore Near Earth Asteroids with 1000 cooperative autonomous spacecrafts [19]. ESA has plans to use swarm intelligence for its APIES mission [20]. Agent based models for satellite constellations have been explored by the Princeton Satellite Systems, which has made a MATLAB toolbox called TeamAgent for the purpose [17]. Their agents represent software and remote terminals connect these with the hardware. The study demonstrated four MAS architectures (top-down coordination, central coordination, distributed coordination and fully-distributed coordination) and compares their performance (evaluated by CPU workload and communication effort) for simple functions such as de-orbiting and reconfiguration. Similar work has been done at CNES, where fully-distributed coordination for Earth observation satellite constellations with limited communication were investigated in detail for Fault Detection Identification and Recovery (FDIR) based on an intricately defined trust and collaboration model and subsequently defined protocols [21].

This paper addresses the capability of satellite clusters, and the newly developing fractionated spacecraft, to perform collision avoidance manoeuvres via distributed and autonomous path planning and control, in the event of directed or random kinetic-impact threats. It enumerates several strategies of manoeuvres in response to different mission constraints. For example, one of the mission constraints could be to not lose communication links between the entities at any time in the manoeuvre. In the path-planning approach proposed in this paper, the satellites determine their states based on artificial potential functions with coefficients determined through equilibrium shaping. The principles of swarm intelligence are used by each satellite in the cluster to react to an external threat.

The approach has several advantages over previously published literature. The path planning and target assignment method is completely autonomous and distributed, no captain or leader in the cluster is required. It is scalable to tens and hundreds of satellites in a cluster with global convergence to target formation for any symmetrical geometry. Asymmetrical geometries have also been demonstrated (even within this paper), however, is susceptible to local minima resulting in erroneous potentials and target formations. Target acquisition is not dependent on initial conditions or states. The algorithm in each satellite's software uses only relative states of the cluster elements to determine its target state.

3. Scatter manoeuvre implementation

In our approach, the satellite cluster has been treated as a multi-agent system. While the proposed algorithms can be scaled up for any number of satellites, symmetric geometries and inter-satellite ranges, for the purpose of the demonstrations within this paper, the cluster of satellites has a limited number of heterogeneous satellites, a few candidate topologies, a predefined communication and sensing range and distributed processing/computing abilities. Agent based autonomy has four levels of hierarchy [17] and only completely distributed systems have been addressed in this paper. The rules of path-planning or determination of target states are those of swarm intelligence where scientists have attempted to copy the simple rules used by individual agents such as birds or bees within large flocks because these rules result in evolved, coherent behaviour of the entire swarm as a whole. Some simple examples are: an agent must "avoid" other agents that are too close, must "copy" the general direction of movement of the swarm, must move such that its "view" is not blocked by another agent, must try to remain close to the "centre" of the swarm and so on [18]. These agents use self-organizing, decentralized control mechanisms and form flexible, robust and scalable systems that respond well to rapidly changing environments. They do not require global communication and rely on individual simplicity to respond to local incontingencies either due to the environment or due to the activities of other agents.

3.1. Artificial potential functions for kinematic path-planning

The concepts described in this section are applicable to both homogenous and heterogeneous (e.g. fractionated spacecraft) satellite clusters. The "intelligence" of the satellites (agents in a multi-agent system) is a kinematic model which gives each satellite in the cluster the ability to determine its target velocity vector as a response to its environment, real-time targets at every control cycle. The kinematic model comprises of artificial potential functions (APF) which can be programmed into each satellite's software and use only pre-defined constants and relative states of the other entities in its environment as inputs. APFs can be derived from a general class of attraction/repulsion functions (depending on the polarity) used to achieve swarm aggregation [23,24]. These functions are odd and of the type $g(y) = -y[g_a(|y|) - g_r(|y|)]$, where $g_a(|y|)$ is the attracting function, $g_r(|y|)$ is the repelling function and 'y' is the distance between the satellites. For each $g_r(|y|)$ and $g_a(|y|)$, there exists a $J_r(|y|)$ and $J_a(|y|)$, such that $\nabla J_r(|y|) = y g_r(|y|)$ and $\nabla J_a(|y|) = y g_a(|y|)$, where $J(|y|)$ is called the artificial potential function.

A very common example of $g(y)$, or a satellite's velocity field, is as follows:

$$g(y) = -y[a - b\, exp^{-(\|y^2\|/c)}] \tag{1}$$

There exists a unique distance δ such that $g_a(\delta) = g_r(\delta)$, which means that the equilibrium condition of zero relative velocity occurs at only one unique distance between two satellites. Thus, if such functions are defined for all pairs of satellites in a formation, there can be only a unique geometry possible at the equilibrium condition. Theoretical studies on stability analysis have demonstrated convergence and an analytical value for time of aggregation and maximum size of the swarm can also be calculated [24].

Just as pairs of satellites are modelled to be specific distances apart in Eq. (1), a food source (or any entity to be attracted to) can be modelled as an attractor and a physical kinetic threat (or any entity to stay away from) can be modelled as a repellent. Some typical potential functions for such sources are as follows [24,25]:

- Linear: $\sigma(y) = a_\sigma{}^T y + b_\sigma$
- Quadratic: $\sigma(y) = (A\sigma/2)\|y - c\sigma\|^2 + b_\sigma$
- Gaussian: $\sigma(y) = \frac{A\sigma}{2}\, exp\left(-\frac{\|y - c\sigma\|^2}{l\sigma}\right) + b_\sigma$

The target velocity vector of a satellite at a relative position 'y' with respect to a source c_σ is the differential of the selected potential function. For more than one source, the target velocity of a satellite will be the summation of the contribution of each potential function. For example, if all sources are modelled as Gaussians, then the total potential on any satellite due to the contribution of N such sources is

$$\sigma(y) = -\sum_{i=1}^{N} \frac{A_\sigma^i}{2}\, exp^{\left(-(\|y - c_\sigma^{i2})/l_\sigma^i\right)} + b_\sigma \tag{2}$$

An example of the Gaussian velocity fields, derived from these potentials, is shown in Fig. 1.

According to the above theory, a set of equilibrium functions corresponds to a unique geometry for the satellite cluster. Therefore, the vice versa must also be true: Any geometry for a cluster can be achieved by using

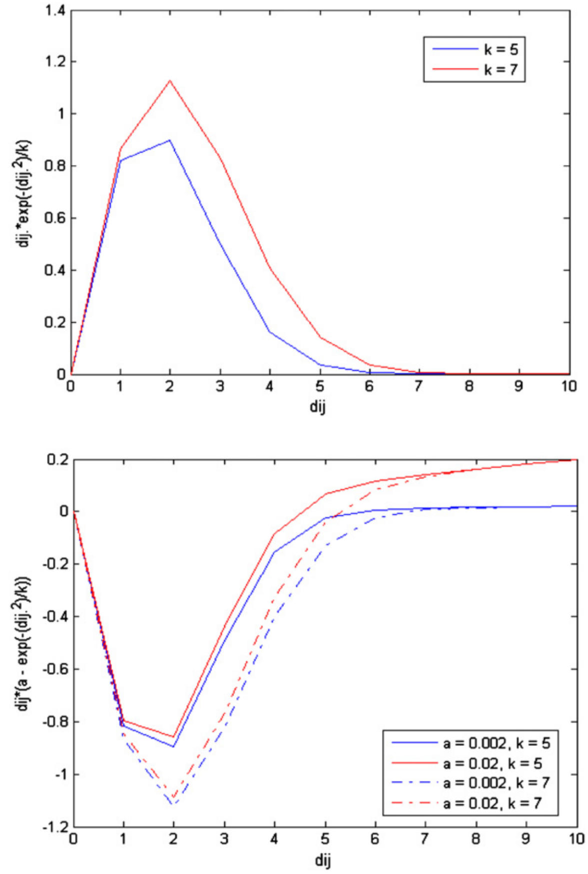

Fig. 1. Velocity fields using exponential functions. X-axis (d_{ij}) = distance between the satellite and the source, Y-axis = velocity of the satellite according to Eq. (2) where $l\sigma = k$ in the figure and $A\sigma = 1$ (scaling factor).

appropriate potential functions and calculating the coefficients (i.e., the free parameters) correctly, for each satellite. Thus, this method can be applied to swarm aggregation, social foraging and most importantly in our case, formation flying [25]. While the above theory was originally developed for robots, the first instance of its adaptation to suit satellite clusters was implemented at the Advanced Concepts Team in the European Space Agency [26–28]. Homogenous satellites modelled as points in space were initiated at random states and were successfully able to gather at particular geometries without colliding with each other by using the simple rules of "dock" (modelled as an exponent), "gather" (modelled linearly) and "avoid" (modelled as an exponent). Up to hundreds of homogenous satellites were able to achieve the required formation within 60,000 s, where each satellite was programmed to achieve target states using specific potential functions that followed the above rules. The coefficients or free parameters for the APFs were calculated by the technique called "equilibrium shaping" [27], where in a set of linear equations for the total velocity field of each satellite were equated to zero, to solve for the free parameters at the equilibrium condition of the system (minimum potential state). The equilibrium condition in turn was pre-set as per the desired formation or relative geometry of the cluster.

The current study builds on past literature by introducing the concept of an external threat, capable of destroying or degrading the satellites by kinetic impact, and studies the ability of the satellites to avoid the threat while also avoiding each other to prevent collisions. The threat is modelled using artificial potential functions, as a moving target that has to be avoided. The potential function used for the threat is modelled as an exponential potential function and the target velocity of a satellite 'i' at a given instant of time, as response to the threat, is given by

$$v(i) = A*\overline{a}*exp\left(-\frac{dij^2}{K}\right) \tag{3}$$

In Eq. (3), d_{ij} is the distance between the threat 'j' and the satellite 'i' at the given instance of time, K is a function of the sensing radius of the satellite, $\overline{a}$ is the unit vector in the direction the satellite is programmed to move in order to avoid the threat and A is a scaling factor. $\overline{a}$ can be either in the opposite direction of the approaching threat (which is not a smart strategy because threats are usually faster than the escape speed of the satellite) or in the perpendicular direction to the approaching threat.

Fig. 2 shows a simple example of a simulation of four heterogeneous satellites that were originally in a rhombus formation on the $z=0$ plane. The rhombus has sides of 6 m each, the angles are 60° and 120° and the centroid lies at (0,0,0). The red circles show the original configuration of the cluster and the blue circles the final configuration. The green line shows the trajectory of the threat, approaching from the positive Z direction (black arrow), moving at a velocity of 1 m/s. The Gaussian distribution for the APF is chosen as a function of the sensing radius of the satellites because the satellites will be able to sense the threat only when it is within their sensing radii. Assuming a sensing radii of 10 m, the 3σ point of the Gaussian distribution lies at 10 m. Since $K=2\sigma^2$, K(at $\sigma=20/3$) in Eq. (3) is calculated to be 22.22 m. The potential functions (APF) used by each satellite to determine its target velocity in Fig. 2 were that of the threat (exponential, $K=22.22$, $A=40$, $\overline{a}$ in the direction opposite to the threat) and linear attraction and exponential repulsion as given in Eq. (1) ($b=20$, $c=10$) for the individual satellites. 'a' in Eq. (1) is calculated from the equilibrium shaping formula i.e., by setting total velocity for each satellite at the equilibrium condition to zero. The equilibrium condition is determined by the final geometry to be acquired by the satellites in terms of their relative states. For a rhombus with length 6 m, 60–120° angles, the distance between any pair of satellites is 10.39 m between the apex/farthest satellites and 6 m for all other pairs. The 6 m inter-satellite distances were chosen based on typical 10 cm CubeSAT high bandwidth, inter-satellite communication ranges. Setting the velocity of Eq. (1) to zero for all satellites, $a(i,j)$ for the ith–jth satellite pair is given by:

$$a(i,j) = b*exp\frac{-del(i,j)^2}{c} \tag{4}$$

where $del(i,j)$ is the distance required between the ith and the jth satellite.

Once the parameters (i.e., the full matrices a, b and c) are determined by solving Eq. (4), each satellite can calculate its target velocity given by the summation of Eqs. (1) and (3) using the appropriate values from the determined parameters. When the threat is within 10 m of the cluster, it moves directly away from the threat, as is seen in Fig. 2—the path planning algorithm is determined through Eqs. (1) and (3). When the threat is greater than 10 m away from the cluster, only Eq. (1) governs the satellite's target velocity and so its rhombus configuration is established again within an error of 1 μm. In a real world mission, the constant parameters/matrices can be calculated beforehand, depending on the desired configuration of satellites and required aversion to the threat, and stored within the software of every satellite. The satellites can use these constant parameters and the real-time relative states of the other satellites and threat (as per their sensing capabilities) and calculate their target velocities real-time. Alternatively, if the mission designer wishes to keep the cluster configuration an open variable, appropriate APF equations and a linear solver can made available to each satellite, so that they may each determine the parameters as per the required geometry and threat condition (e.g. multiple threats vs. single threat). The system is therefore adaptable, dynamic and completely decentralized.

In the scheme described above, the cluster has about 10 s to react to the approaching threat, given that the threat moves at a velocity of 1 m/s and the sensing radii is 10 m because it is relying completely on the individual sensors of its satellites to detect the approaching threat. Real-world threats (esp. kinetic missiles) are much faster, so in order to successfully avoid them, the satellites with CubeSAT capabilities must either have a threat sensing radii of 50 m or more, or must rely on a warning signal from a ground station. From the next section onward, all modelling has taken into account a warning from the ground station to all the satellites. At the

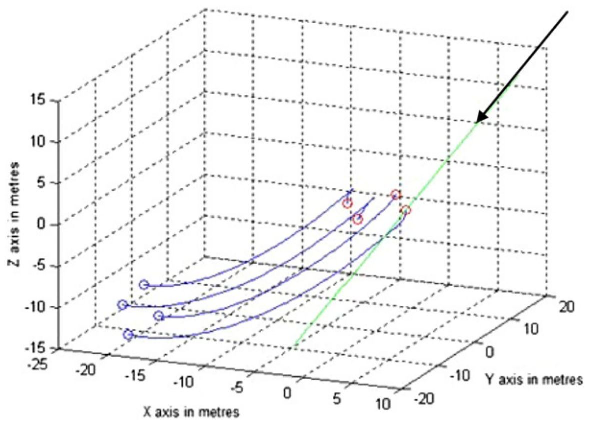

Fig. 2. Trajectory of a satellite cluster (blue lines) in the event of an approaching threat (green line with an arrow to indicate direction). The red circles show the original configuration of the cluster and the blue circles the final configuration. Note that one of the satellites would have been hit, had the cluster not moved. (For interpretation of the references to colour in this figure legend, the reader is referred to the web version of this article.)

time of the warning, the ground is assumed to provide the following information to the satellites: 3D position of the threat at time of warning, its velocity vector and the time stamp of dispatching this information. Once warned, all the satellites set the threat sensing radii values within their APF software equal to their distance from the threat (at the time when the warning was broadcast) within their internal kinematic model and then begin to set target states accordingly ($v(i)=v(\text{Eq. }(1))+v(\text{Eq. }(3))$). It is has been assumed in this paper that the threat moves in a straight line, so the satellites are able to forward propagate in time every subsequent position of the threat, hence 'knows' where it is. The model proposed can be easily adapted for real time missions by either having the ground station send out the approximate trajectory of the threat and/or send the threat state periodically, such that the clusters may use the most recent state to calculate their target behaviours. When the threat has passed, the ground station is expected to broadcast the 'safe' flag and the satellites can reset the sensing radii values in the APF software back to the true sensing radii (i.e., 10 m as demonstrated in Fig. 2). Thus, the ground station forecast allows the satellites to have a virtual sensing radii for the purpose of usage within the kinematic model, which gives the cluster more time to react to the threat and which would not have been possible if the satellites relied only on physical sensors.

For demonstration of the proposed algorithms, heterogeneous satellites in the cluster are defined in terms of CubeSat mass, power and subsystem requirements ($\sim$7 kg, 3CU, 5 W per satellite), while the advancing threat is defined in terms of its approach velocity, head-time and circular area probable (CEP). The satellite model chosen is similar to the one used in NASA Ames GeneSAT. Algorithms have been demonstrated using CubeSAT capabilities to keep with ESA's increased interest in small satellites (e.g. the NanoSat study performed at the CDF [22]).

3.2. Dynamics and controls for actuation

The example in the previous section demonstrated a simple kinematic model for determining target states of a satellite cluster treated as a swarm. The dynamical system is defined by adding a control feedback, based on the kinematic model to track the desired velocities, to the solution of the Hill–Clohessy–Wittshire equations [29] at the mission altitude. The Hill's equations for eccentric orbits (Eq. (5)) and their analytical solution (with an eccentric anomaly $H(v)$) are given in [30]. While it is certainly possible to obtain the full solution as the dynamic system, it is beyond the scope of what this paper aims to demonstrate hence for the sake of simplicity, circular orbits are considered. The cluster is assumed to be in Low Earth Orbit (LEO), 7000 km from the Earth's centre with a period of 6.74e−4 days and an angular velocity (n) of 1.078e−3 rad/s. Since the orbit is assumed to be circular, the three HCW equations simplify to Eq. (6) and an analytical solution is also available.

$$\frac{d}{dt}\begin{bmatrix}\dot{x}\\ \dot{y}\\ \dot{z}\end{bmatrix} = -2\begin{bmatrix}0 & -\dot{v} & 0\\ \dot{v} & 0 & 0\\ 0 & 0 & 0\end{bmatrix}\begin{bmatrix}\dot{x}\\ \dot{y}\\ \dot{z}\end{bmatrix} - \begin{bmatrix}0 & -\dot{v} & 0\\ 0 & -\dot{v}^2 & 0\\ 0 & 0 & 0\end{bmatrix}\begin{bmatrix}x\\ y\\ z\end{bmatrix}$$

$$-\begin{bmatrix}0 & -\dot{v} & 0\\ \dot{v} & 0 & 0\\ 0 & 0 & 0\end{bmatrix}\begin{bmatrix}x\\ y\\ z\end{bmatrix} + n^2\left(\frac{1+e\cos v}{1-e^2}\right)X\begin{bmatrix}2x\\ -y\\ -z\end{bmatrix} + \begin{bmatrix}a_x\\ a_y\\ a_z\end{bmatrix} \tag{5}$$

$$\ddot{x}_i - 2n\dot{y}_i - 3n^2x_i = \frac{u_{x_i}}{m_i}$$
$$\ddot{y}_i + 2n\dot{x}_i = \frac{u_{y_i}}{m_i}$$
$$\ddot{z}_i + n^2z_i = \frac{u_{z_i}}{m_i} \tag{6}$$

In Eq. (6), $u(x_i)$, is the control force for the x component of the ith satellite and so on for $u(y_i)$ and $u(z_i)$. The control force depends on the control scheme selected for the dynamic system. For the purpose of swarm aggregation in space, the following feedback control schemes have been demonstrated in literature [26]:

- Q-Guidance controls via Cross Product Steering Law (CPSL)
- Q-Guidance controls via Velocity to be Gained Law (VTBG)
- Sliding mode controls (SMC)
- Artificial Potential approach controls (APC)

The results show that the delta-V spent via VTBG and SMC are the lowest for the average satellite in the swarm. For the purpose of demonstrations in this paper, a simple proportional (to velocity) controller is used and the control acceleration can be written as

$$u_i = k(\dot{x}_i - v_i) + \ddot{x}_i - a_{in} \tag{7}$$

where $\dot{x}_i$ is the kinematic velocity and $\ddot{x}_i$ the kinematic acceleration obtained from the kinematic swarm model described in the previous section, v_i is the actual dynamic velocity of the satellite in Hill's frame and a_{in} are the inertial forces. The $(\dot{x}_i - v_i)$ term is called velocity-to-be-gained, v_g. The parameter k is analogous to the known steering laws [31]. For example, if k goes to infinity, the control strategy is to thrust in the direction of the velocity to be gained vector regardless of the contribution of the uncontrollable term, $\ddot{x}_i - a_{in}$. In our simulations using the dynamic framework, the control accelerations were determined from the kinematic target velocities (Eq. (7)) and resulting dynamic positions and velocities were calculated using a simple ODE 45 solver.

In real missions, as with the kinematic model, all parametric constants, a linear and differential equation solver will be available within the software of each satellite. Each satellite will therefore be able to determine its kinematic target velocity in the same way as described in Section 3.1 real-time, find the acceleration required by solving the control equation in Eq. (7) and then determine its dynamic target state by solving the differential equation.

Technological feasibility of the proposed algorithms and strategies have been benchmarked using technologies available to small satellites, in terms of mass, thrust, etc.

Actuation feasibility of the control strategy is tested in simulation using numbers from available/potential CubeSat propulsion capabilities which puts a cap on the maximum thrusting ability and maximum fuel spent by the spacecraft. Both electrical and chemical propulsion systems are being developed for CubeSATs. The electrical systems [32] offer very low thrust of ~70 μN but a high specific impulse of >3500 s within 0.5 kg of propulsion systems. The chemical systems [33,34] offer a higher thrust of 2–10 mN per thruster (4 thrusters per cube) but a total delta-V of 35 m/s for the same system mass of 0.5 kg. For the simulations enumerated in the forthcoming sections, when the control accelerations required were greater than that possible to actuate by the thrusters, the thrust was capped to the maximum thrust available, i.e., 1.4 mm/s^2 for chemical propulsion or 14 μm/s^2 for electrical propulsion. Initial simulations showed that electric propulsion was not capable of thrusting enough to help the cluster manoeuvre out of threat's way with more than 1 m of miss distance using the path planning strategies demonstrated in the paper. All the results thus demonstrate the performance of a chemical propulsion system.

4. Demonstration of scatter manoeuvre strategies

The following section describes various strategies that can be taken by a multi-satellite homogenous or heterogeneous (e.g. fractionated spacecraft) cluster in order to approach a threat approaching it using various types of artificial potential functions (APF), calculated using equilibrium shaping (ES). The threat is modelled as a point object travelling in a straight line, but as explained in Section 3.1, it is possible to model and implement more complex trajectories of approaching threats. The strategies have been designed in response to specific mission requirements and flexibility allowed of the geometric configuration of the cluster during the scatter manoeuvre. The various strategies are compared to each other in terms of metrics: probability of success without loss of long-term functionality, minimum distance of approach between the satellites and the threat, delta-V spent and time required to return to normal operations. Since each strategy is unique to a mission requirement, the metrics should be traded with mission-level metrics to understand and compare value of the strategies. In themselves, the metrics are not a measure of comparative value of the strategies. Further, the mission requirements and the scatter strategies are chosen as examples to demonstrate the applicability of the APF and ES to distributed scatter manoeuvres to several mission constraints. More requirements, strategies and functions are certainly possible for larger clusters of more (tens or even hundreds) satellites in any symmetrical geometrical configuration. The strategies described and compared in this section and the associated potential functions used to model swarm behaviour and determine the kinematic target velocities are listed below.

1. Strategy 1: scatter and gather
   Mission requirement: Collision avoidance from the threat by direct exit from a predefined threat ellipse and a subsequent gather strategy that activates after the ground station warning is switched off—'safe' flag signalled.
   APFs used for scatter: Lennard Jones potential function, Scatter potential function, viscosity function
   APFs used for gather: Gather potential, avoid potential, dock potential
2. Strategy 2: adaptation to threat by moving cluster centroid
   Mission requirement: Collision avoidance from the threat with a shift in the formation centroid of the cluster allowed, however control over the relative geometry of the cluster needs to be maintained throughout the scatter manoeuvres.
   APFs used: Gather potential, avoid potential, threat potential
3. Strategy 3: Adaptation to threat by fixed cluster centroid
   Mission requirement: Collision avoidance from the threat with the formation centroid of the cluster required to be fixed at all times however no control over the relative geometry for the cluster is required.
   APFs used: Gather potential, avoid potential, dock potential, threat potential
4. Strategy 4: Mix-and-match demonstration
   Mission requirement: Collision avoidance from threat by scattering such that a shift in the formation centroid of the cluster is allowed, i.e., Strategy 2 after being warned by the ground station, followed by the gather strategy of Strategy 1 after the ground station warning is switched off—'safe' flag signalled. Strategy 4 is not a novel strategy, instead demonstrates the ability of the proposed methodology to improvise with the usage of artificial potential functions to build cluster behaviours as desired.
   APFs used for scatter: Gather potential, avoid potential, threat potential
   APFs used for gather: Gather potential, avoid potential, dock potential.

All the simulations were implemented in a dynamic Hill's frame as described in Section 3.2 with a limit on the maximum control accelerations allowed to actuate the guidance and navigation, as determined by the dynamic model using APFs. The maximum control accelerations are determined by nominal CubeSAT chemical thruster forces applied to a typical CubeSAT mass. Since the space environment has some other random forces such as solar radiation, air drag, lunar gravity and solar gravity, white noise of the amplitude of $1e-6$ [35] was added to the Hill's equations of Eq. (7). All the strategy demonstrations described have used 4–6 satellites in the specific-geometry cluster as a proof of concept in simulation, but it is, in theory possible to scale the number of satellites up to hundreds in a symmetric swarm and the methodology would still hold good [36]. The only requirement would be to recalculate the constant parameters (much larger matrices) such as those in Eq. (4) for the geometry desired with the satellite swarm, and to make them available to all the satellites in the cluster—the rest of the methodology, i.e., to calculate kinematic states and then dynamic states, remains the same. Since the constant parameters and the dynamic accelerations can be determined for both homogenous and heterogeneous clusters, it is easily possible to adapt these strategies described for fractionated spacecraft for increasing number of components and complexity. Heterogeneous cluster simulations have been successfully implemented in this regard and also described below.

4.1. Strategy 1: scatter and gather

This is the simplest strategy using distributed decision-making and artificial potentials and has been demonstrated in the example below using a rhombus cluster formation. The mission scenario considered is: Four satellites in a rhombus formation on the plane $z=0$ that has sides of 6 m each, the angles are 60° and 120° and the centroid lies at (0,0,0). At $t=0$, the ground station warns the satellites of an approaching threat and requires them to move out of a sphere of radius 20 m centred at (0,0,0). In response to this scenario, the potential functions used to calculate the satellite target states for the scatter process after being warned by the ground station are as follows:

- *Lennard Jones potential function* determines the attraction–repulsion between the satellites. If $V(r)$ is the LJ potential between two bodies at a separation 'r', then its derivative, $v1(r)$, will be the velocity of a single satellite, as explained in Section 3.1.

$$V(r)=\varepsilon\left[\left(\frac{\sigma}{r}\right)^{12}-2\left(\frac{\sigma}{r}\right)^{6}\right] \tag{8}$$

$$v1(r)=\frac{12\varepsilon}{r}\left[\left(\frac{\varepsilon}{r}\right)^{12}-\left(\frac{\varepsilon}{r}\right)^{6}\right] \tag{9}$$

  As per the LJ molecular theory, the attraction is very strong when r is not much larger than σ, but after a certain distance this force fades to zero. This means that two molecules, or in our case two satellites, interact strongly only when their mutual distance is within a certain value, thus explaining the reason why we called this potential local. The stable arrangement of two molecules interacting with each other is such that they respect the mutual target distance σ. In the above equations, ε is the depth of the potential well, which accounts for the attractiveness and stability of the minima located at distance σ. It is set at 0.1 for this simulation [28]. We set σ to be 10.59 m for the furthest two satellites in the rhombus and 6 m for all other pairs. The important feature of this potential is that the lattice is formed on the basis of positional information only: no communication is needed.
- *Scatter potential function* forces the satellites to move radially outward from the centre of the danger sphere i.e., the avoid region specified by the ground station when forecasting the warning.

$$v2(r)=d[R^2-r^2] \tag{10}$$

  For the purpose of the scatter potential, a Cartesian coordinates are transformed to a new spherical coordinate system whose centre is equal to the centre of the danger sphere ($R=20$ m in our case). In Eq. (10), $v2$ represents the radial component of the velocity of a single satellite in the new coordinate system, x the radial position of the satellite, and d the scaling factor. The angular components of the $v2$ are set to zero. The avoid region can be extended from a sphere to any other shape by modifying Eq. (10) accordingly.
- *Viscosity function* forces the satellites to stop motion when they reach the danger sphere's surface. Once the swarm converges to its final configuration, the gravitational influence of the planet tends to disrupt the formation, therefore the satellites need to use their thrusters to maintain their relative positions. Simulations show that the satellites actually oscillate around their equilibrium points, thus wasting propellant. A solution to this problem can be found again with physical considerations. The physical analogy is to imagine the satellites immersed in a viscous medium, such as for example air or some liquid. Therefore, the mathematical expression of the velocity due to the viscosity potential is as follows:

$$vis=\begin{cases} K\exp^{(-\xi/2)} & \text{if } \xi<D \\ 0 & \text{otherwise} \end{cases} \tag{11}$$

This virtual viscosity is applied to the satellite's velocity if ξ i.e., the difference between the required radial position and the actual radial position is less than a threshold value, i.e., the satellite is almost at target. In our simulation, $D=0.5$ m, which means that when the satellite is within 0.5 m of the surface of the danger sphere. Once the viscosity is known, velocity can be calculated as

$$v3=-\xi\dot{x} \tag{12}$$

Here, $\dot{x}$ is the actual velocity of the satellite. If the danger sphere is a shape different from a sphere, Eq. (11) will also be modified accordingly.

The kinematic target velocity of each satellite in this strategy for the scatter is calculated at each control cycle by the summation of $v1$, $v2$ and $v3$. Since the satellites have the constants stored within their software beforehand, it is easy to determine all the velocities based on the relative distances to the other satellites and the threat. Results of this simulation, without and with a cap (due to actuation limits of hardware) on control acceleration in the Hill's frame, are shown in Fig. 3. The control profiles are shown in Fig. 4 that indicates that thrust at their maximum available thrust for 1500–2000 s after which the controls die down because the satellites have reached their targeted sphere surface. The delta-V spent is ~1.8 m/s which proves this strategy to be extremely delta-V and thrust expensive.

Once the satellites have scattered and the threat has passed over, the ground station is assumed to broadcast the information ('safe flag') to the satellites. When the satellites receive this information, a different strategy is used to model the return of the satellites to their original positions. The artificial potential functions used for this

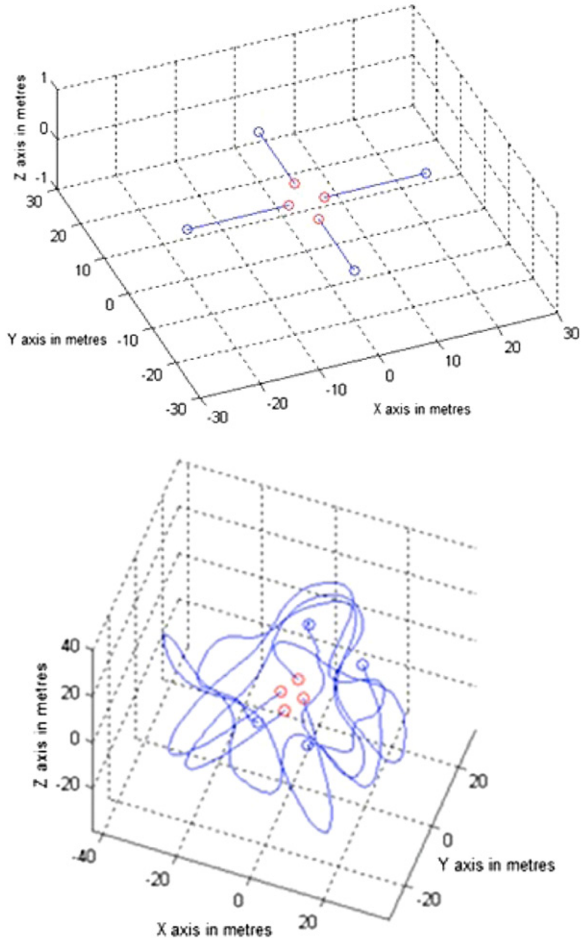

Fig. 3. Strategy 1 results: (Top) Trajectories of the satellites when there is no constraint on the control acceleration. (Bottom) Trajectories of the satellites when control acceleration of each satellite is capped at 1.4 m/s^2. The red circles show the original configuration of the cluster and the blue circles the final configuration. (For interpretation of the references to colour in this figure legend, the reader is referred to the web version of this article.)

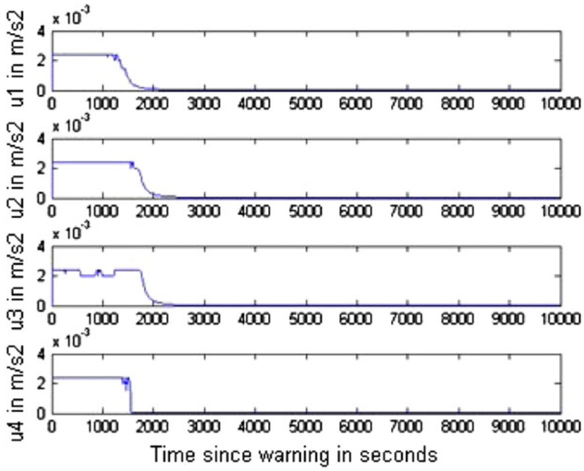

Fig. 4. Control acceleration (thrusting) profiles for Strategy 1 with an imposed maximum control acceleration of 1.4 m/s^2 per satellite (RMS = 2.1 m/s^2).

return phase, per control cycle, to determine their target velocities for each satellite are as follows:

- *Gather potential* introduces 4 different and unique global attractors towards the sinks of the desired formation, which in this demonstration are the nodes of the rhombus in Hill's frame. Therefore each agent has to know at each time where is the position of each point of the final formation to be achieved. The expression for this kind of behaviour is defined as

$$v1(i,t) = -c(i,t) * dx(i,t) \tag{13}$$

  Eq. (13) is the velocity of the ith satellite with respect to an attractor "t" (unique target, since the cluster is heterogeneous), with $dx(i,t)$ as the distance between the ith satellite and its target and c is the scaling factor determined via equilibrium shaping.

- *Avoid potential* establishes a keep-away relationship between two different agents that are in proximity with each other. In such a case a repulsive contribution will assign to the desired velocity field a direction that will lead both the two agents away from each other. The expression that describes the assigned velocity of a single satellite i with respect to another satellite j for this kind of behaviour is given below:

$$v2(i,j) = -dx(i,j)\left[b(i,j) * exp\left(\frac{-\|dx(i,j)\|}{k2}\right)\right] \tag{14}$$

  In this equation, $x(i,j)$ is the distance between the two agents that are proximate and $k2$ describes the sphere of influence of this contribution (within 3ό as described in Section 3.1), i.e., the distance at which this behaviour would have a non-negligible effect. "b" is calculated from the equilibrium shaping.

- *Dock potential* expresses the local attraction of each agent towards each sink i.e., the final locations of the cluster's satellites which in this demonstration are the nodes of the rhombus in Hill's frame. The component of the desired velocity field due to this behaviour has a non-negligible value only if the agent is in the vicinity of the sink. The parameter $k3$ determines the radius of the sphere of influence of the dock behaviour. The velocity of a satellite "i" with respect to a target position "t" for this potential is given as

$$v3(i,t) = -dx(i,t)\left[d(i,t) exp\left(\frac{-\|dx(i,t)\|}{k3}\right)\right] \tag{15}$$

  in which again $x(i,j)$ is the distance between the two agents that are proximate and $k3$ describes the sphere of influence of this and 'd' is calculated from the equilibrium shaping.

To calculate the constant parameters, the total satellite velocity for each satellite ($v1+v2+v3$) is set to zero, for the equilibrium geometrical configuration of a rhombus at $z=0$. 'c' is set at 3.214e−3 for required target and 'd' at 40. '$k2$' and '$k3$' to 6 for an assumed sensing radii of 6 m. To calculate the required 'b', Eq. (16) is used for the satellites at the furthest ends of the rhombus and Eq. (17) is used for all other pairs of satellites.

$$b(i,j)=\frac{3c+3*d(i,j)*exp(-l^2/k3)+\sqrt{3}*d(i,j)*exp((-3l^2)/k3)-\sqrt{3}*b(i,j)*exp((-3l^2)/k2)}{exp(-l^2/k2)} \tag{16}$$

$$b(i,j)=\frac{3c+3*d(i,j)*exp(-l^2/k3)}{exp(-l^2/k2)} \tag{17}$$

In both the above equations, it must be noted that the calculation is an approximation to the original ones used in simulation. For the original calculations, each x, y and z components of the velocity were set to zero, in which case there would be 3 independent equations to solve for instead of 1 for each heterogeneous pair of satellites, after assuming equal values for 'c' and 'd'. For the full calculation, the 'l' in Eqs. (16) and (17) would be replaced by the difference between the x coordinates, y coordinates and z coordinates for each set of satellites. As noted, the more heterogeneous and fractionated the cluster, the more the number of constants to be determined, but easily possible given a linear solver.

The desired kinematic velocity of any satellite in the re-gather phase expressed as a sum of all three velocities, $v1$, $v2$ and $v3$ for all the targets and is calculated and actuated in the dynamic frame at every control cycle. The re-gather strategy has a delta-V of ~0.5 m/s per satellite and takes 900–1200 s to complete.

4.2. Strategy 2: Adaptation to threat by moving cluster centroid

This is a simple strategy in response to a mission scenario which requires the entire cluster to move out of the path of approach of the threat while maintaining relative geometry between the component satellites. The strategy has been demonstrated using four satellites in a rhombus formation on the plane $z=0$ that has sides of 6 m each, the angles are 60° and 120° and the centroid lies at (0,0,0). At $t=0$, the ground station is assumed to warn the satellites of an approaching threat and requires them to move out of the direction of approach of the threat. There is with no restriction on the overall position of the cluster during scatter, however, fixed relative distances is required to be maintained i.e., cluster geometry remains intact (in this case a rhombus of side 6 m with a 60–120° angle between its sides). Like in Strategy 1, four satellites are considered however unlike Strategy 1, an approaching threat is modelled as per Eq. (3) where $\overline{a}$ is set to make the cluster move in the direction of the approaching threat i.e., away from the threat. The threat is modelled to move at a velocity of about 1 km/s. The original position of the cluster had the rhombus on the $z=0$ plane with the centroid at (0,0,0) but the final position is about a 1 km away as seen in Fig. 5.

The potential functions used to calculate the kinematic target velocities for each satellite are those of "Gather" and "Avoid" (i.e., the attraction–repulsion function in Eq. (1)) and "Threat" (Eq. (3)), as described in the previous sections. Fig. 5 shows the trajectories of the satellites for a simulation when the ground station issued the warning 2000 s before one of the satellites was to be hit by the threat. In spite of such an early warning, the miss distance was calculated as 7 m and an average delta-V of 1.6 m/s. This is because by escaping in the direction opposite to the threat, the satellites thrust at their maximum but their velocity is naturally not enough to escape the velocity of the threat. As a result, it is only when the threat is very close that the satellites move *out* of its way. This is clearly not a good strategy because no matter how early the warning is issued, the delta-V would be wasted only to make the formation accelerate but not move out the threat's way. The warning is switched off at the 600th second as seen in the control profiles of Fig. 6 where the second leg of maximum thrust is to bring the satellites back to their relative geometry within a simulation time of 1000 s. The average error in geometry, calculated as the average RMS error per inter-satellite distance, is 8 cm after the simulation is completed.

Strategy 2 can be modified such that in the threat potential function in Eq. (3) is perpendicular to the direction of approach of the threat (modify $\overline{a}$). Since the ground station informs the cluster of the velocity vector of the threat, the satellites can calculate an infinite number

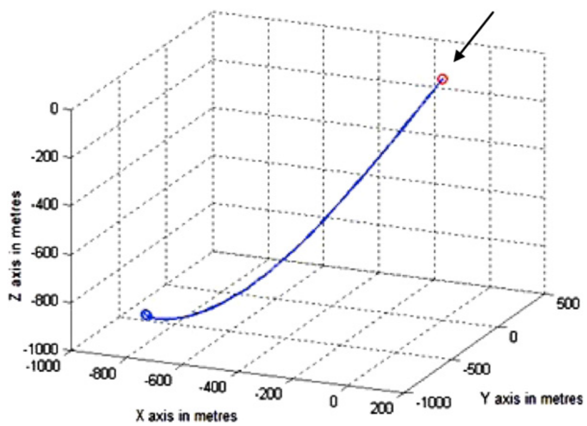

Fig. 5. Trajectory of the rhombic cluster in Strategy 2 when it moves opposite to the approaching threat (direction marked by an arrow). The axes are the X-, Y-, Z-axis in the right-handed coordinate system in metres. The red circles show the original configuration of the cluster and the blue circles the final configuration. (For interpretation of the references to colour in this figure legend, the reader is referred to the web version of this article.)

of vectors perpendicular to that vector and randomly pick any one of the solutions, or additional mission constraints may exist to the direction of movement. The other parameters of the threat potential function remain the same and so do the other potential functions i.e., Gather and Avoid. The simulation is run for several different time periods as shown in Table 1. In the table, 'Headtime' is the time available between when the ground station issued the warning and when one of the satellites is calculated to be hit by the threat i.e., the time that the cluster has to avoid being hit. 'Warning off time' is the time elapsed after the warning was issued at which the warning is switched off. The difference between 'Headtime' and 'Warning off time' is the time when the cluster has to continue its scatter manoeuvre to avoid the threat. Average miss distance is the average distance of closest approach between the threat and any satellite. Velocity of attack is the RMS velocity of the threat in the Hill's frame. Error is the formation error calculated as the average of the RMS errors between what the inter-satellite distances are at the end of the simulation and what they should be as per mission geometry.

Fig. 7 (top) shows a test simulation where the green line represents the approaching threat—direction marked with an arrow. Fig. 7 (bottom) shows Sim # 2, Sim #3, Sim #4 in Table 1. It can be clearly seen from the table that the miss distance is a function of only headtime (given the maximum thrust of the satellites is limited), irrespective of the velocity of attack. Also, given more simulation time, the error of formation i.e., the average RMS error per inter-satellite distance, reduces. For example, the error reduces by 16 cm when the simulation is run for 200 s more—compare Sim #2 and Sim #3 in Table 1.

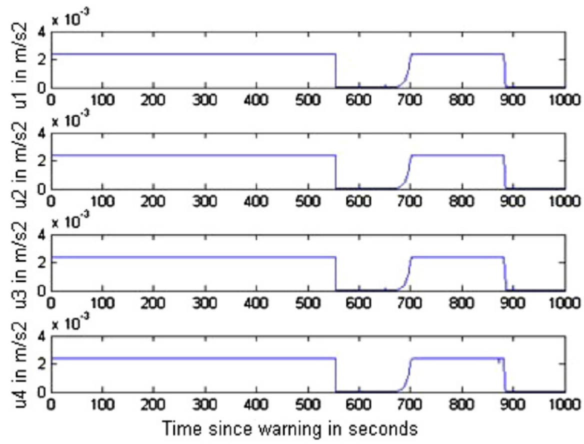

Fig. 6. Control acceleration (thrusting) profiles of each of the 4 satellites in Strategy 2 when it moves opposite to the approaching threat (direction marked by an arrow).

4.3. *Strategy 3: Adaptation to threat by fixed cluster centroid*

This strategy is demonstrates the cluster scatter manoeuvre using APFs for a mission that requires a fixed cluster centroid before and after the passage of the threat but does not put any constraints on the relative configuration of the satellites. The cluster geometry is allowed

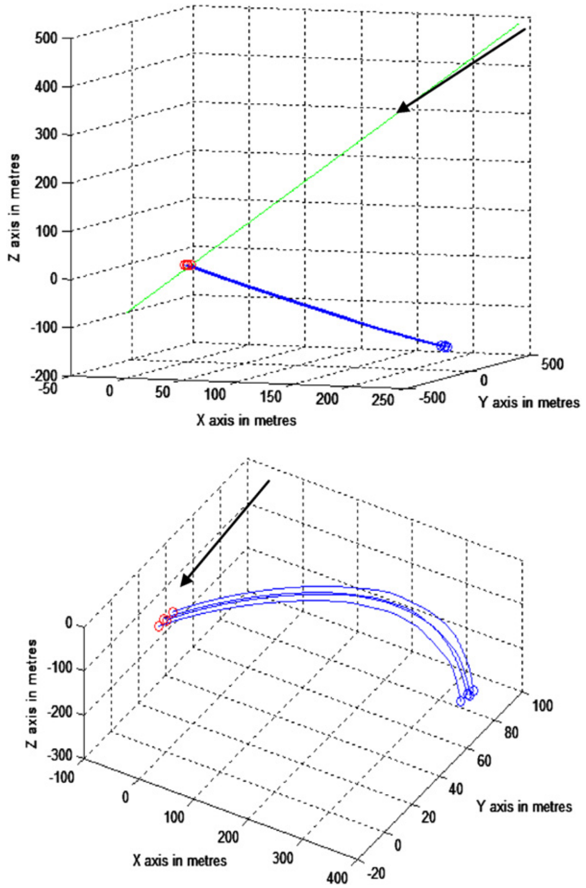

Fig. 7. Trajectory of the rhombic cluster in Strategy 2 when it moves perpendicular to the approaching threat (direction marked by an arrow) and control acceleration limited to 1.4 m/s^2. The red circles show the original configuration of the cluster and the blue circles the final configuration. (For interpretation of the references to colour in this figure legend, the reader is referred to the web version of this article.)

Table 1.
Comparison between different metrics (described in the text) in Strategy 2.

Sim #	Headtime (s)	Velocity of attack (m/s)	Warning off time (s)	Simulation time (s)	Error (cm)	Average miss distance (m)
1	50	1	100	200	4	4
2	200	1	400	500	45	45
3	200	1	400	700	29	45
4	200	1000	400	700	22	45

to be broken during the scatter manoeuvre but the cluster is required to return to where it started in the Hill's frame after the threat has passed. The strategy is demonstrated using six satellites in a hexagonal formation with a side length of 6 m. The potential functions used to calculate the kinematic target velocities for each satellite are: "Gather" (Eq. (13)), "Avoid" (Eq. (14)), "Dock" (Eq. (15)) and "Threat" (Eq. (3)) potentials. The equilibrium shaping formula will now require a solution of 18 equations similar to the one below in Eq. (18) (obtained by summing Eqs. (13)–(15) and setting to 0), for each satellite $i=1$–6 and for 3 x–y–z dimensions.

$$c(i,t)*dx(i,t)+dx(i,j)\left[b(i,j)*\exp\left(\frac{-\|dx(i,j)\|}{k2}\right)\right] + dx(i,t)\left[d(i,t)\exp\left(\frac{-\|dx(i,t)\|}{k3}\right)\right]=0 \tag{18}$$

Once all the constant matrices are calculated, they are made available to all the satellites for scatter manoeuvring in this specific mission scenario (Strategy 3). As mentioned before, when the ground station warning is received, each satellite uses these constants and the relative states of all the other satellites and the approaching threat to calculate its target state at every control cycle and actuates it in the dynamic environment. In the simulation, the warning was forecast by the ground station 500 s before the threat was to hit one of the 6 satellites and turned off 130 s after the warning was turned on. Fig. 8 shows the trajectory of the satellites in blue and the trajectory of the threat (with an arrow for direction) in green. The control profiles in Fig. 9 show the satellites thrusting at maximum for almost the entire period when the warning was on. After it is switched off, they began thrusting again after a time lag in order to come back to their original positions. The entire simulation lasted 430 s, the average delta-V spent per satellite was 0.86 m/s and the minimum distance of closest approach with the threat was 62 m. Again, had the threat velocity been modelled such that the satellites escaped opposite to the direction of approaching threat instead of

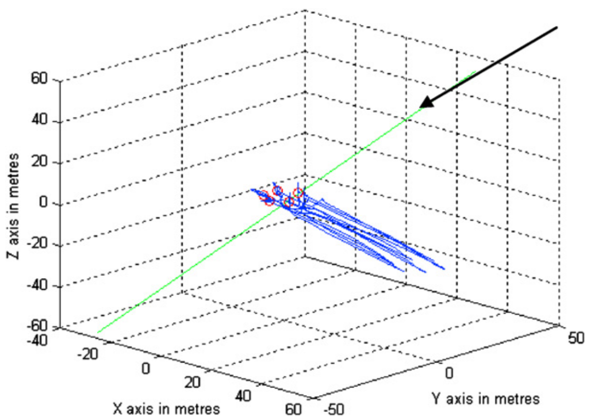

Fig. 8. Trajectory of the hexagonal cluster in Strategy 3 when it moves perpendicular to the approaching threat. The red circles show the original configuration of the cluster and the blue circles the final configuration. (For interpretation of the references to colour in this figure legend, the reader is referred to the web version of this article.)

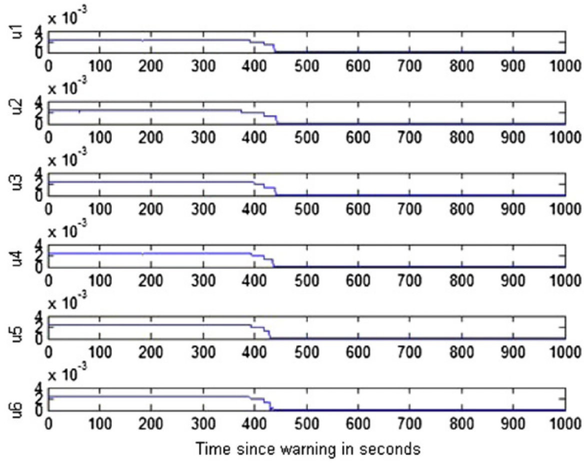

Fig. 9. Control acceleration (thrusting) profiles of each of the 6 satellites in Strategy 2 when the cluster moves perpendicular to the approaching threat (direction marked by an arrow).

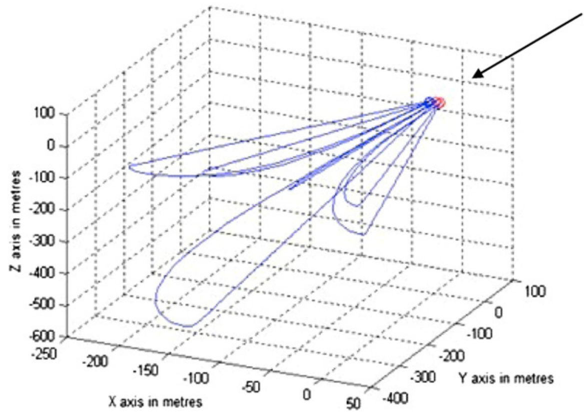

Fig. 10. Trajectory of the hexagonal cluster in Strategy 3 when it moves perpendicular to the approaching threat (direction marked by an arrow). The axes are the X-, Y-, Z-axis in the right-handed coordinate system. The red circles show the original configuration of the cluster and the blue circles the final configuration. The arrow shows the direction of approaching threat. (For interpretation of the references to colour in this figure legend, the reader is referred to the web version of this article.)

perpendicular, the delta-V spent for the same warning and higher simulation time (1000 s) is higher (1.3 m/s) for a minimum miss distance of 9 m. The trajectory is shown in Fig. 10.

An important consideration in this strategy is that when the satellites scatter, they go hundreds of metres away from each other as seen in Fig. 10, which could be orders of magnitude greater than the range that the inter-satellite communications are designed to operate at. To effectively use this strategy, the subsystems must be designed to account for this drop in bandwidth during the scatter manoeuvre or switch to a different communication system if such an opportunity arises. Maintaining a good communication link is especially important for fractionated spacecraft where there may be elements that critically need other elements to operate. That this strategy also causes the satellites to fly out of each others' sensing radii is not a hindrance to navigation because all satellites are programmed to swarm back toward the predefined centroid and avoid potentials will automatically kick in when they sense each other in close vicinity.

4.4. Strategy 4: Mix-and-match demonstration

This strategy demonstrates that the artificial potential functions or even full individual strategies described in all the previous sections can be combined in convenient ways to design different target behaviours of swarms of satellites as per different mission requirements. Strategy 4's demonstration does not use any new strategy or APF and is simply Strategy 2 followed by the re-gather part of Strategy 1. A four satellite rhombic formation is used. The potential functions (APF) used to calculate kinematic target velocities are the attraction-repulsion potential of Eq. (1) and the threat potential of Eq. (3), (satellites are forced to move in a direction perpendicular to threat), when the warning is switched on and the Gather, Avoid and Dock potentials (Eqs. (13)–(15)), when the warning is deactivated by the ground station. The simulated trajectory of the satellites is shown in Fig. 11. The allowed head-time for the simulation is 300 s and the warning is turned off 500 s after being turned on. Total simulation time was 2000 s, which gave an average delta-V of 0.9 m/s per satellite and a minimum distance of closest approach as 33 m for a threat approach velocity of 1 m/s.

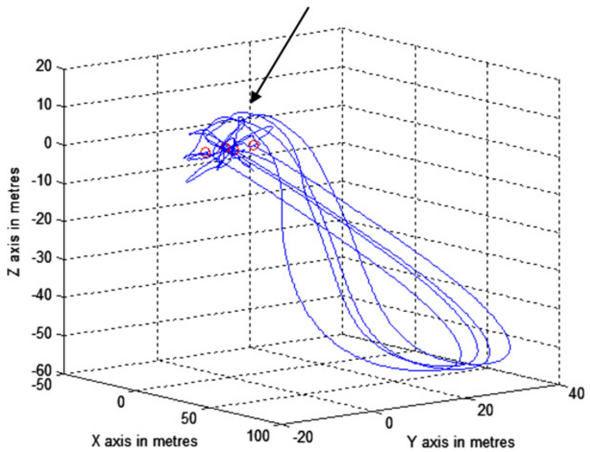

Fig. 11. Trajectory of the rhombic cluster in Strategy 4 when it moves perpendicular to the approaching threat. The red circles show the original configuration of the cluster and the blue circles the final configuration. (For interpretation of the references to colour in this figure legend, the reader is referred to the web version of this article.)

4.5. Summary of APF and ES based demo-strategies

The strategy to use in a particular scenario depends on the mission requirements and the scenario itself rather than how the strategies perform with respect to each other. The four scatter manoeuvre strategies discussed from Sections 4.1 to 4.4 are compared in Table 2. Strategies 2 and 3 has been divided into two parts: one for movement parallel to direction of threat and two, for perpendicular movement i.e., different vectors $\overline{a}$ in Eq. (3). The metrics considered in Table 2 are average time (averaged over all satellites) required to reconfigure and return to normal operations, average delta-V per satellite required for the scatter manoeuvre and the minimum distance of closest approach of the threat with any satellite. Since we have used the ground station information to turn the threat warning on and off and the satellites have responded to this information (Except Strategy 1 where the satellites are not made aware of the threat parameters), the average time required for the reconfiguration depends on the amount of time the satellites have to react to the threat (headtime) and the time after which the GS switches off the warning (warning off time). Similarly, the miss distance depends only on the headtime and the direction of escape. Delta-V spent depends on the average time required for the reconfiguration and the maximum thrust available to the satellites. Probability of success of the scatter manoeuvre approach without loss of long-term functionality can be calculated as a function of the miss distance and the error ellipse of the threat destruction trajectory. Since a point threat moving in a straight line has been assumed for the purpose of the paper, the calculations for error ellipses and therefore probabilities of success, although possible, are beyond the scope of the paper's goals. Initial simulations showed that the strategies (apart from the gather strategy which is very delta-V expensive) depend on the input parameters and mission scenarios, but in themselves, are not very different from each other in terms of resource expenses. Hence, for the purpose of demonstrating the applicability of AP functions to determine satellite kinematics for collision avoidance manoeuvres in a dynamic on-orbit environment, varying mission scenarios have been selected and consistent performance has been shown for appropriately selected strategies and APFs.

Mission requirements apart from the ones described in this section are also possible by designing strategies to respond to them and appropriate APFs for the strategies. It is also possible to program the satellites with many modular strategies and APFs such that when the ground

Table 2.
Comparison of the strategies described on the basis of different metrics (described in the text).

Strategy #	Average time (s)	Average delta-V (m/s)	Minimum miss distance (m)
Strategy 1 (scatter+gather)	3000+1000	1.8+0.5	N/A (equal to circle of threat)
Strategy 2 (parallel)	900	1.6	7 (for headtime=200 s)
Strategy 2 (perpendicular)	700	0.4	45 (for headtime=200 s)
Strategy 3 (parallel)	1000	1.3	9 (for headtime=500 s)
Strategy 3 (perpendicular)	430	0.86	62 (for headtime=500 s)
Strategy 4 (mix and match)	2000	0.9	33 (for headtime=300 s)

station issues the threat warning (approach information of the kinetic impact of the threat), it will also issue a command to use one or a combination of the strategies along with information on the required final geometrical configuration. Each satellite can solve the linear equation system of equilibrium shaping using the commanded APFs and inter-satellite distances for the required geometry, find the constant parameters and then use the constant parameters at every subsequent control cycle with the relative states of the other satellites to find its target state. The ground station may also update the threat trajectory at any point, requiring a simple recalculation of APF constants as described above and in Section 3.1.

5. Conclusion and future work

Satellite clusters aim to achieve, similar to autonomous multi-robot/agent-systems, increased robustness (by taking advantage of parallelism and redundancy), as well as provide the heterogeneity of structures and functions required to undertake different activities in hazardous and uncertain environmental conditions such as those present in space. They are designed to require minimal communication from the ground and within the agents, to reduce computation loads and save on time spent to find optimal solutions via a centralized agent. The case of a homogenous or heterogeneous satellite cluster, even the new paradigm of fractionated spacecraft, reacting to a kinetic impact threat has been taken up in this paper. The models suggested in this paper have demonstrated only position control of the satellites. Additional attitude control can be easily implemented by solving the 7 ES equations (for position – x, y, z – and quaternion – $q1, q2, q3, q4$) per satellite instead of 3 for only position – x, y, z – and then actuating both attitude and position control.

The applicability of artificial potential functions to navigate large satellite clusters in the event of an external kinetic impact threat by scatter manoeuvring their elements in a dynamic on-orbit environment (approximated by the Hill's frame in this paper) has thus been clearly demonstrated using several strategies. The strategy and APFs chosen would depend on mission constraints because that influences the absolute and/or relative placement of satellites required by the cluster. All the strategies are scalable and APFs can be easily calculated and equilibrium shaping control implemented for symmetric geometries of tens or hundreds of spacecrafts. A small number, 4 and then 6, was chosen to demonstrate the concept and larger clusters would only require calculation of a larger number of parameters in the equilibrium shaping equation. This will not affect the reaction time or CPU load after a threat is declared because they need to be solved only once, depending on the cluster and mission requirements, and uploaded onto the satellites (or if required, calculated within satellites) before they even begin scatter operations. Thus, by tweaking local parameters, it is possible to exhibit intelligent emergent coordination at the global level. For example, if the fractionated spacecraft has different functionalities (such as wireless power transfer) embedded or faces a change in mission needs, the strategies can be adapted accordingly.

Since the equilibrium shaping technique is based on minimizing the virtual potential of each satellite in order to bring them to a halt at the required relative configuration, the biggest limitation of the technique is its tendency to get stuck in local virtual potential minima which need not necessarily correspond to the correct geometry. This limits its application to very large satellite swarms in an asymmetric geometry since these are most susceptible to local minima errors. For such systems, global evolutionary path planning techniques using artificial neural networks, although never demonstrated in space, is theoretically a better approach.

The equilibrium shaping technique for position and attitude control is currently being tested on the SPHERES satellites aboard the International Space Station [16]. Algorithms for a triangular formation of three satellites starting at random initial locations have been successfully demonstrated on the SPHERES simulator. Hardware tests are scheduled to be run on the SPHERES nanosatellites in microgravity this year to demonstrate feasibility for satellite clusters in the real space environment as well as robustness to excess disruption and noise, not modelled in the simulation. Results from the SPHERES test sessions will be made available in a later publication.

Acknowledgements

The authors are grateful to Dario Izzo and Jurgen Leitner at the Advanced Concepts Team (ACT), ESTEC, for very useful discussions on the topic of the paper and to Prof. Olivier de Weck at MIT for suggesting the scatter manoeuvre problem as an important one in distributed space systems. The primary author would like to thank the International Relations Department of ESA for making her internship at ESTEC possible in the summer of 2010 and for funding her research stay in the ACT. Special thanks to the Taiwan National Space Organization and the National Central University for funding the author's travel to Taiwan to present the first draft of this paper at the International Workshop on Satellite Constellations and Formation Flying in November 2010.

References

[1] O. Brown, P Eremenko, The Value Proposition for Fractionated Space Architectures, AIAA-2006-7506, San Jose, CA, 2006.
[2] D.M. LoBosco, G.E. Cameron, R.A. Golding, T.M. Wong, The Pleiades fractionated space system architecture and the future of national security space, presented at the AIAA Space, Anaheim, CA, 2008.
[3] Charlotte Mathieu, Assessing the Fractionated Spacecraft Concept, Massachusetts Institute of Technology, Cambridge, Massachusetts, USA, 2006.
[4] ESA Internal Report on Fractionated Spacecraft, European Space Agency, Noordwijk, The Netherlands, ESA/ESTEC contract 22258/09/NL/AF, February 2010.
[5] Proba Mission Page on the European Space Agency website. [Online]. Available: 〈http://www.esa.int/esaMI/Proba/SEMXZ5ZVNUF_0.html〉.
[6] L. David, Space Debris: A Growing Challenge, American Institute of Aeronautics and Astronautics, Aerospace America, October 2009, pp. 30–36.
[7] L. Grego, Short History of US and Soviet ASAT Programs, Union of Concerned Scientists, April 2003.

[8] A. Richards, T. Schouwenaars, J.P. How, E. Feron, Spacecraft trajectory planning with avoidance constraints using Mixed-Integer Linear Programming, J. Guidance Control Dyn. 25 (4) (2002).

[9] Y. Kim, M. Mesbahi, F.Y. Hadaegh, Multiple-spacecraft reconfiguration through collision avoidance, bouncing, and stalemate, J. Optim. Theory Appl. 122 (2004) 323–343.

[10] J. Mueller, R. Larsson, Collision avoidance maneuver planning with robust optimization, presented at the ESA Guidance, Navigation and Control Conference, Tralee, Ireland, 2008.

[11] R. Larsson, J. Mueller, S. Thomas, B. Jakobsson, P. Bodin, Orbit constellation safety on the PRISMA in-orbit formation flying testbed, presented at the ESA Formation Flying Symposium, The Netherlands, 2008.

[12] G.L. Slater, S.M. Byram, T.W. Williams, Collision avoidance for satellites in formation flight, J. Guidance Control Dyn. 29 (5) (2006).

[13] J.B. Mueller, A multiple-team organization for decentralized guidance and control of formation flying spacecraft, presented at the AIAA 1st Intelligent Systems Technical Conference, Chicago, IL, 2004.

[14] Shawn B. McCarnish, Marcello Romano, Simon Nolet, Chritine Edwards, David W. Miller, Ground and flight testing of multiple spacecraft control on spheres during close proximity operations, J. Spacecr. Rockets 46(6) (2009).

[15] J.G. Katz, A. Saenz-Otero, D.W. Miller, Development and demonstration of an autonomous collision avoidance algorithm aboard the ISS, in: Aerospace Conference, IEEE, 2011, pp. 1–6.

[16] Alvar Saenz-Otero, et al., Distributed satellite systems algorithm maturation with SPHERES aboard the ISS, presented at the International Astronautical Congress, Glasgow, Scotland, 2008.

[17] T. Schetter, M. Campbell, D. Surka, Multiple agent-based autonomy for satellite constellations, Artif. Intell. 145 (2003) 147–180.

[18] E. Bonabeau, M. Dorigo, G. Theraulaz, Swarm Intelligence: From Natural to Artificial Systems, Santa Fe Institute Studies on the Sciences of Complexity, 1999.

[19] S.A. Curtis, J. Mica, J. Nuth, G. Marr, M. Rilee, M. Bhat, ANTS (autonomous nano-technology swarm): an artificial intelligence approach to asteroid belt resource exploration, in: Proceedings of the International Astronautical Federation, 51st Congress, 2000.

[20] P D'Arrigo, S Santandrea, The APIES mission to explore the asteroid belt, Adv. Space Res. (2006).

[21] G. Bonnet, C. Tessier, Multi-agent collaboration: a satellite constellation case, in: Proceedings of the Fourth Starting AI Researchers' Symposium, 2008.

[22] NanoSat: Development of a Highly-Capable, Modular Miniaturised Platform, CDF Study Report CDF-84(A), European Space Agency, Noordwijk, The Netherlands, 2009.

[23] V. Gazi, K. M. Passino, Stability analysis of social foraging swarms: combined effects of attractant/repellent profiles, in: Proceedings of the 41st IEEE Conference on Decision and Control, Las Vegas, NV, USA, 2002.

[24] V. Gazi, K.M. Passino, Stability analysis of swarms, IEEE Trans. Automat. Control 48 (4) (2003).

[25] V. Gazi, B. Fidan, Y.S. Sanay, Aggregation, foraging, and formation control of swarms with non-holonomic agents using potential functions and sliding mode techniques, Turk. J. Electr. Eng. 15 (2) (2007).

[26] M. Ayre, D. Izzo, L. Pettazzi, Self assembly in space using behaviour based intelligent components, in: Proceedings of the TAROS: Towards Autonomous Robotic Systems, London, United Kingdom, 2005.

[27] D. Izzo, L. Pettazzi, Autonomous and distributed motion planning for satellite swarm, J. Guidance Control Dyn. 30 (2) (2007).

[28] Carlo Pinciroli, Mauro Birattari, Elio Tuci, Marco Dorigo, Evolving a Collective Consciousness for a Swarm of Pico-Satellites, Advanced Concepts Team Ariadna Report Ariadna Final report ID 07/8101 under contract 20765/07/NL/CB, European Space Agency, Noordwijk, The Netherlands, 2008.

[29] W.H. Clohessy, R.S. Wiltshire, Terminal guidance system for satellite rendezvous, J. Aerosp. Sci. 27 (1960) 653–658.

[30] M. Tillerson, G. Inalhan, J. How, Co-ordination and control of distributed spacecraft systems using convex optimization techniques, Int. J. Robust Nonlinear Control 12 (1) (2002) 207–242.

[31] R.H. Battin, An Introduction to the Mathematics and Methods of Astrodynamics, New York, USA, 1987.

[32] P. Lozano, D. Courtney, On the development of high specific impulse electric propulsion thrusters for small satellites, in: Proceedings of the Symposium on Small Satellite Systems and Services, Funchal Madeira, Portugal, 2010.

[33] The CubeSAT Propulsion module from Delft University. [Online]. Available: 〈http://www.lr.tudelft.nl/live/pagina.jsp?id=b01f8765-4b61-4c5a-8f20-96e5871934f5&lang=en〉.

[34] K. Sarda, C.C. Grant, S. Eagleson, D.D. Kekez, R. Zee, Canadian advanced nanospace experiment 2 orbit operations: two years of pushing the nanosatellite performance envelope, in: Proceedings of the Symposium on Small Satellite Systems and Services, Funchal Madeira, Portugal, 2010.

[35] Jian Ma, Formation Flying of Spacecrafts for Monitoring and Inspection, SpaceMaster Master Thesis, Lulea University of Technology, Department of Space Science, Kiruna, 2007.

[36] D. Izzo, L. Pettazzi, Equilibrium shaping: distributed motion planning for satellite swarm, in: Proceedings of the 8th International Symposium on Artificial Intelligence, Robotics and Automation in Space, 2005.